Soil water evaporation during the dry season in an arid zone

Nurit Agam (Ninari),[1] Pedro R. Berliner, and Abraham Zangvil

Jacob Blaustein Institute for Desert Research, Ben-Gurion University of the Negev, Sede-Boker Campus, Israel

Eyal Ben-Dor

Remote Sensing and GIS Laboratory, Department of Geography, Tel-Aviv University, Ramat Aviv, Tel-Aviv, Israel

[1] The objective of this study was to assess the relative magnitude of latent heat flux density over a bare loess soil in the Negev desert throughout the dry season, during which the atmospheric models usually assume the lack of latent heat flux. The measurements were carried out in the northern Negev, Israel, over a bare loess soil, during nine 24-hour field campaigns throughout the dry season of 2002. In addition to a micrometeorological station that was set up in the research site, an improved microlysimeter was installed. The representativity of the microlysimeter was assessed by comparing its surface temperature to that of the surrounding surface using thermal images acquired on an hourly basis during several campaigns. It was found that although the water content of the uppermost soil is significantly lower than the wilting point, for which most of the commonly used meteorological models would assume no latent heat flux, the latter was ~20% of the net-radiation during the night and 10–15% during the day. It is therefore concluded that latent heat flux plays a major role in the dissipation of the net radiation during the dry season in the Negev desert. *INDEX TERMS:* 1866 Hydrology: Soil moisture 1878 Hydrology: Water/energy interactions; 3322 Meteorology and Atmospheric Dynamics: Land/atmosphere interactions; *KEYWORDS:* energy partitioning, latent heat flux, bare soil

Citation: Agam (Ninari), N., P. R. Berliner, A. Zangvil, and E. Ben-Dor (2004), Soil water evaporation during the dry season in an arid zone, *J. Geophys. Res.*, *109*, D16103, doi:10.1029/2004JD004802.

1. Introduction

[2] Land surface processes in general, and the energy partitioning at the soil surface in particular, play an important role in global and mesoscale studies. These processes are usually integrated as subsets (or submodels) of global and mesoscale models. During the last decade a number of land surface models have been developed [*Yang et al.*, 1998]. One of their main tasks is to describe the patterns of radiant energy dissipation at the land-atmosphere interface, which above bare soil are determined by the moisture content of the soil surface. It is therefore reasonable that the quality of land surface models should be judged by the accuracy with which they compute the aforementioned soil water content [*Irannejad and Shao*, 1998]. The moisture level of the soil is the result of the interaction of atmospheric variables (radiation, temperature, wind speed, etc.) with the transport of mass and energy in the soil. The transport of mass and energy in the soil (and consequently evaporation of water from the soil surface) has been intensively studied, and various formulations and numerical solutions based on the general theory of *Philip and de Vries*

[1957] have been presented [e.g., *Milly*, 1982, 1984; *Kondo et al.*, 1990; *Scanlon and Milly*, 1994; *Parlange et al.*, 1998; *Qin et al.*, 2002]. The use of such detailed descriptions is not appropriate for large-scale modeling due to the vast amount of field data required [*Yang et al.*, 1998] and the intense computational efforts involved. This problem is usually circumvented by parameterizing the evaporation flux as a function of the potential evaporation and some easily computed index of surface moisture [*Shao and Henderson-Sellers*, 1996].

[3] One approach to the parameterization method is the supply and demand formulation, according which the actual evaporation rate is computed from

$$E = \min\{E_p, E_c\} \qquad (1)$$

in which E, E_p and E_c (W m^{-2}) are the actual evaporation, the potential evaporation and the maximum rate at which the soil profile can transport water to the soil surface, respectively. It should be noted that even though this approach is simpler than simultaneously solving the coupled equations for mass and energy in the atmospheric boundary layer and in the soil, the drawbacks mentioned previously apply to the computation of E_c. The computation of the actual evaporation using formulae of the type

$$E = \beta E_p \qquad (2)$$

[1]Also at Department of Geography and Environmental Development, Ben-Gurion University of the Negev, Beer-Sheva, Israel.

in which β depends explicitly on the soil water content is therefore favored and widely used [*Shao and Henderson-Sellers*, 1996].

[4] *Carlson et al.* [1984] defined β as:

$$\beta \equiv \frac{R_b}{R_b + R_s} \approx \frac{\theta}{\theta_{sat}}, \quad (3)$$

where R_b (m s^{-1}) and R_s (m s^{-1}) are the atmospheric and soil resistances respectively and θ and θ_{sat} the actual and field saturation values of volumetric soil water content. β varies from 0 (absolutely dry surface) to 1 (saturated surface), and its value is required for each grid point in the model. *Carlson et al.* [1984] suggested deriving β from the remotely sensed surface temperature and thermal inertia. The simplicity of the approach and the possibility to obtain maps of β using remotely sensed data are two attractive features of this approach. The linearity of the dependence appears, on the other hand, to be an oversimplification. As a result, an improved formulation, which accounts for the field capacity and the wilting point moisture contents of the soil, was incorporated in the land-surface model that is used as part of the fifth generation Mesoscale Model (MM5), jointly developed by the Pennsylvania State University and the National Center for Atmospheric Research. In this model, β is computed using [*Chen and Dudhia*, 2001]

$$\beta = \frac{\theta - \theta_w}{\theta_{ref} - \theta_w}, \quad (4)$$

where θ is volumetric water content, and θ_{ref} and θ_w are field capacity and wilting point.

[5] In this case as well, β varies linearly from 0 (no evaporation) to 1 (evaporation at a rate that equals the potential evaporation). This formulation is based on the implicit assumptions that the soil moisture content does not drop below the wilting point (as β cannot be negative), and therefore latent heat flux vanishes when the soil moisture content reaches the wilting point. Mesoscale models of this type were developed mostly for temperate climate zones [*Bougeault*, 1991], for which these assumptions are probably valid. Their applicability to other climatic regions should be considered with great care. A point in case would be desert areas, for which it has been shown that the soil dries well below the wilting point [*Boulet et al.*, 1997].

[6] The detailed description of land-surface processes is, however, not limited to mesoscale models, but is also a key feature of global circulation models. It was found that the exchanges of momentum, heat and moisture between the atmosphere and the Earth's surface have a fundamental influence on the dynamics and thermodynamics of the atmosphere [*Chen and Dudhia*, 2001]. Evidence from atmospheric general circulation model experiments suggests that the climate is sensitive to variations in evaporation from the land surface [*Schmugge and Andre*, 1991]. As the accuracy of the general circulation models response is dominated by subgrid-scale parameterizations of inputs and parameters of land surface processes [*Avissar and Pielke*, 1989; *Hu and Islam*, 1997; *Robock et al.*, 1998; *Sridhar et al.*, 2003], the accuracy and sensitivity of these inputs are of great importance.

[7] The parameterization method described above (i.e., parameterizing the actual evaporation according to the soil water content) is, however, very crude [*Blondin*, 1991]. It was found that model simulation results are very sensitive to the soil parameters chosen for assessing β [*Shao and Henderson-Sellers*, 1996; *Lohmann et al.*, 1998] especially during nighttime [*Irannejad and Shao*, 1998] and when the soil is relatively dry [*Yang and Dickinson*, 1996; *Yang et al.*, 1998]. Notwithstanding the uncertainties of this type of parameterization, it is still widely used [e.g., *European Centre for Medium-Range Weather Forecasts*, 2002].

[8] In general, land surface models differ only slightly from each other, and are all based on different degrees of simplification of the detailed processes [*Yang et al.*, 1998; *Gusev and Nasonova*, 2003]. The urgent need is therefore not to develop "new" land surface models, but to evaluate and test the available models with field data. Moreover, high-quality field data are crucial for improving land surface models [*Yang et al.*, 1998].

[9] Very few data sets that address the problematic environmental conditions stated above are available. Usually, in arid zones, measurements of evaporation are carried during the period during which the soil remains wet in the wake of rainfall events [*Mitsuta et al.*, 1995]. The rationale being that during the dry period evaporation is negligible. Surprisingly, however, diurnal changes in the water content of the uppermost soil layer (with a corresponding latent heat flux density) were monitored in the desert even during the dry season [*Agam (Ninari) and Berliner*, 2004]. The commonly used approach to the parameterization of evaporation discussed previously (equation (2)), may, in these circumstances, lead to significant errors in the assessment of the radiation dissipation patterns in arid zones. The objective of this study was to assess the relative magnitude of latent heat flux density over a bare loess soil in the Negev desert throughout the dry season, during which the atmospheric models usually assume the lack of latent heat flux.

2. Materials and Methods

[10] The measurements were carried out at the Wadi Mashash Experimental Farm in the northern Negev, Israel (31°08′N, 34°53′E; 400 m A.M.S.L., 60 km from the Mediterranean Sea). Rainfall events occur between October and April, and the mean annual rainfall at the farm is 115 mm. Long-term maximum and minimum temperatures are 14.7°C and 4.8°C for January; and 32.4°C and 18.6°C for July, respectively. Class A pan evaporation is 2500–3000 mm per year. The soil is a sandy loam Aridisol (Loess) with 13% clay, 15% silt, and 72% sand.

[11] Data were collected during nine 24-hour field campaigns that took place during the dry season of 2002. A total of 124 mm of rain was recorded during the rainy season of 2001–2002 (prior to the above mentioned measuring period). The first campaign took place 10 weeks after the last rainfall of the 2001–2002 season (29 March, 13.5 mm), and the last one ended about 2 hours before the first rainfall of the next season (30 October). The remaining seven campaigns were randomly spread within these two dates.

[12] During each campaign a micrometeorological station was installed nearby, in a spot in which the fetch in the prevailing wind direction (N-NW) is 200 m and devoid of

vegetation, for continuous measurement of incoming and reflected short-wave radiation with two pyranometers (CM5, Kipp & Zonen); net-radiation (Q-7, Campbell Scientific Inc.); wind speed at four levels (2, 1, 0.5, 0.25 m) with cup-anemometers (014A Met-One); dry- and wet-bulb temperatures at 1m height using a self-designed aspirated psychrometer; soil heat flux at three different locations in the field with heat flux plates (HFT-3, Campbell Scientific Inc.) installed at a depth of 50 mm, and temperature measurements above them at 10 mm intervals, using differentially wired thermocouples. Sensible heat flux was measured with a sonic anemometer (CA27, Campbell Scientific Inc.). Data were measured and collected every 10 s and averaged every 30 min by a data logger (23X, Campbell Scientific Inc.). Additionally, the changes in mass of an improved microlysimeter [*Ninari and Berliner*, 2002] (186 mm diameter and 550 mm of effective depth with an additional 50 mm of polyurethane insulation) were recorded by placing the microlysimeter in a pit and weighing it every
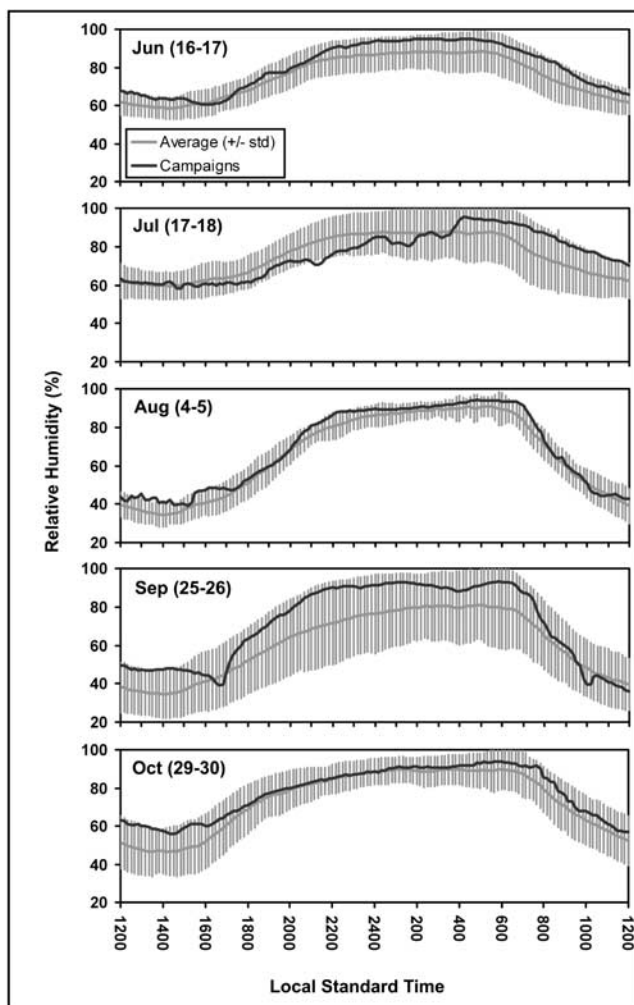

Figure 2. A sample of a thermal image of the microlysimeter and its surrounding, acquired at midnight 26–27 June. The gray level indicates the surface temperature (the brighter the color, the warmer the surface). The dark area around the soil sample is the polypropylene isolation. The two rectangles mark the subsets from which the pixels data were extracted.

half hour. The PVC tube containing the undisturbed soil sample was isolated by polypropylene to avoid lateral heat flux. The scale (AND, maximum weighting capacity of 30 kg) had a resolution of 0.1 gram, which resulted in a resolution of 0.004 mm (equivalent depth of water) or 5.11 W m^{-2} (in energy terms). The output of the scale was registered automatically every half hour by a palm computer (48GX, Hewlett Packard).

[13] Thermal images of the microlysimeter surface together with its surroundings were acquired hourly during several campaigns throughout the season, using a thermal video radiometer (TVR) (INFRAMETRICS 760, 1994). The TVR is highly sensitive in terms of both radiometric temperature and spatial resolutions of the surfaces (±0.05°C and about 0.035 m from height of 20 m, respectively). For the current study, the sensor configuration was optimized to work across the spectral region of 3–14 μm, and the optic configuration enabled a field of view (FOV) of 20° along an instantaneous field of view (IFOV) of 1.8 mRad. Using an onboard internal calibration procedure, the calibration information for each scene of the raw data was recorded on an 8 mm NTSC magnetic tape. Selected images were saved as TIFF files and further processed with image processing software. Analysis and results of five out of the nine campaigns, for which complete sets of data are available, are presented in this paper.

3. Data Analysis and Evaluation

[14] Because of the fact that the dates of the campaigns were selected randomly, it was important to substantiate that they are representative. Data of prime meteorological parameters (i.e., incoming short wave radiation, air temperature, relative humidity and wind speed) were collected from a meteorological station located not far from the research site (and influenced by the same mesoscale con-
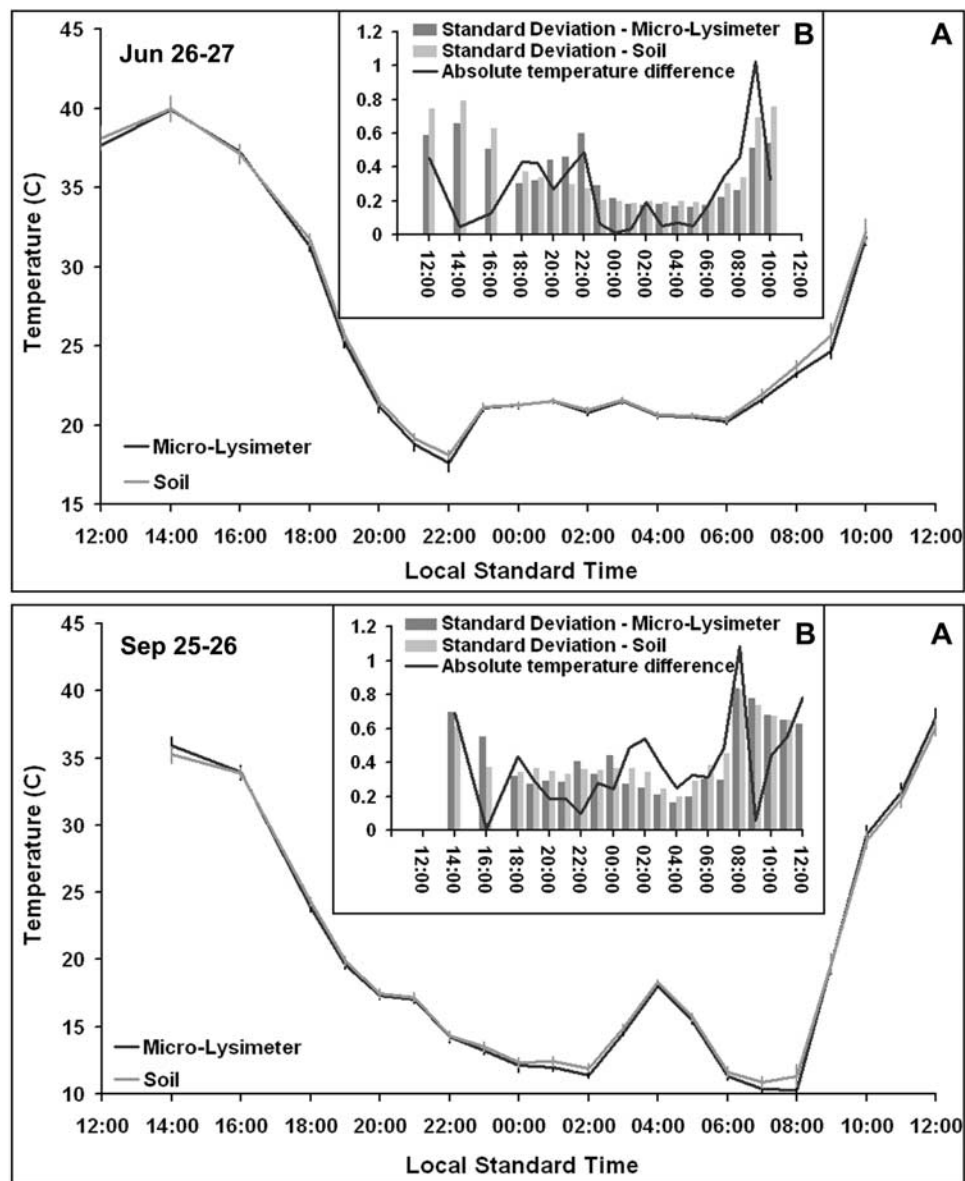

Figure 1. Diurnal changes in the relative humidity measured for each of the campaigns, together with the monthly averages (±1 standard deviation) for the same time intervals are presented. Data were collected from a meteorological station located not far from the research site (and influenced by the same mesoscale conditions).

Figure 3. (a) The daily course of the average temperature (plus or minus standard deviation) of the soil and the microlysimeter, (b) together with the absolute differences between the average temperatures of the soil and the microlysimeter compared to the standard deviation from their averages, for 26–27 June and 25–26 September.

ditions). Data measured during the campaigns were compared to the corresponding monthly averages. Campaign dates in which the values measured were within the range of ±1 standard deviation from the monthly average were considered representative. The diurnal changes in the relative humidity measured for each of the campaigns, together with the monthly averages for the same time intervals are presented as an example in Figure 1. It can be observed that the relative humidity during the campaigns was within 1 standard deviation from the monthly average, except for a few hours at noon of 4 August. Similar patterns were found for the other parameters. It was concluded therefore that the meteorological conditions during these campaigns (of which the dates were randomly selected) are representative of the conditions for the season they stand for.

[15] Various techniques have been used for the measuring of latent heat flux, most of them relaying on micrometeorological methods [*Brutseart*, 1982]. However, in arid environments, the magnitude of latent heat flux during the dry season is very small, a fact that poses some very special technical measurement difficulties [*Ninari and Berliner*, 2002]. In such conditions, even small errors in the parameters used in those methods may result in errors that are of the order of magnitude of the flux itself. Direct methods for measuring latent heat flux are therefore advantageous. Theoretically, the use of a microlysimeter provides an absolute reference for latent heat fluxes, as long as the soil and the heat balance of the microlysimeter are similar to those of the surrounding area. Provided the soil sample is undisturbed and representative of the area, similar temper-

ature profiles will yield equal surface temperatures and hence guarantee that the latent heat fluxes measured with the microlysimeter represent the surrounding soil [*Ninari and Berliner*, 2002].

[16] The representativity of the microlysimeter was tested during several campaigns by comparing its surface temperature to that of the surrounding area. Thermal images of the microlysimeter surface together with its surroundings were acquired hourly. Figure 2 is an example for the acquired images. The representativity of microlysimeters containing undisturbed soil cores usually decreases with time, and in studies with wetting cycles (rain, irrigation) it is common to replace the sample. The disadvantage of this procedure is that it is time consuming and probably affected by the spatial variability of the soil characteristics. In this study, one core was used throughout the whole dry period, and its representativity was assessed shortly after insertion (26–27 June) and toward the end of the measuring season (25–26 September). For the selected campaigns, two subsets of the images (indicated in Figure 2 by the marked rectangles) were produced, representing the surface of the microlysimeter's soil sample and the surrounding soil. The rectangle representing the microlysimeter contained 1071 pixels and the one representing the surrounding soil 33472 pixels, located in an undisturbed area. For each date a set of 20 pairs of subsets were analyzed to compare the surface temperature of the microlysimeter sample to the surrounding soil.

[17] The daily course of the average temperature (plus or minus standard deviation) of the soil and the microlysimeter are presented in Figure 3a. Figure 3b shows the absolute differences between the average temperature of soil and the microlysimeter compared to the standard deviation from their averages. Performance of a goodness-of-fit test showed that the daily course of temperatures of both the microlysimeter surface and the soil surface was similar (For 26–27 June, $\chi^2 = 0.483$, and for 25–26 September, $\chi^2 = 0.271$). During most of the day, the temperature difference between the sample and the soil are less than 0.5°C. A peak difference of 1°C in the morning (9:00 in June and 8:00 in September) is due to a shadow partially falling on the microlysimeter sample for a very short time (because of technical constraints). Moreover, during most of the day, the standard deviations (for both the sample and the soil) are of the same order of magnitude as the temperature differences between them. It can therefore be concluded that the soil sample in the microlysimeter is representative of the surrounding soil, and that the changes in soil water content measured by the microlysimeter are reliable and representative of the changes in the soil water content (and thus the latent heat flux) of the surrounding soil.

[18] In order to assess the relative contribution of the latent heat flux to the energy balance at the soil surface it is, however, important to carefully evaluate the quality of the entire energy balance data. The energy balance at the soil surface is described by

$$NR + G + H + E = 0 \qquad (5)$$

in which *NR* is net-radiation and *G*, *H*, and *E* are soil, sensible, and latent heat fluxes, respectively. All components of the energy balance equation are in (W m^{-2}).
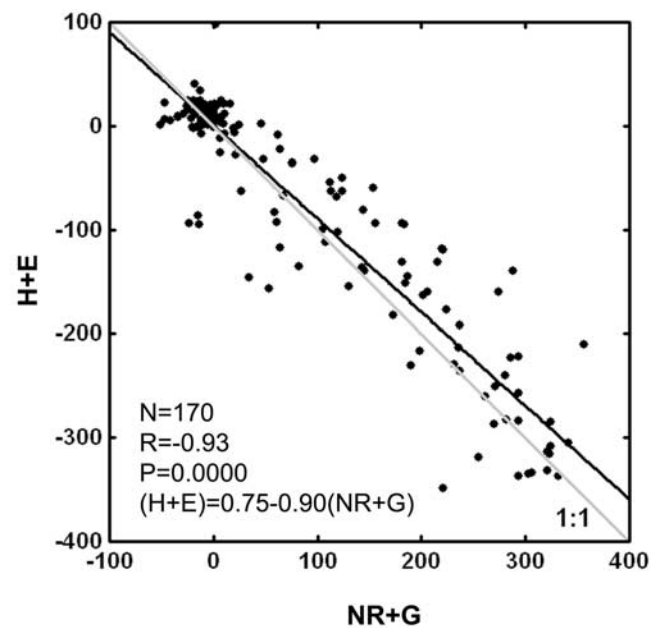

Figure 4. The sum of sensible (*H*) and latent (*E*) heat flux densities versus the sum of net-radiation (*NR*) and soil heat flux density (*G*) together with the corresponding regression analysis. A slope of 0.9 and a correlation coefficient of 0.93 indicate satisfactory closure.

[19] An additional component of the energy balance that should be carefully treated is the soil heat flux. Although its daily mean value is often one or more orders of magnitude smaller than the remaining terms in the energy-balance equation (5), this is not the case during shorter periods of time during which it may be one of the dominating fluxes [*Ninari and Berliner*, 2002]. Soil heat flux plates were inserted in three different places within the measurement site, at a depth of 50 mm. The soil heat flux was computed as the sum of the soil heat flux measured at 50 mm depth (G_p) and the heat stored in the uppermost 50 mm of the soil (G_s):

$$G = G_p + G_s. \qquad (6)$$

The heat storage was computed using

$$G_s = \sum_{j=1}^{5} g_{j+1/2}$$

$$g_{j+1/2} = Cv \frac{\left(T_{j+1}^i + T_{j+1}^{i+1}\right) - \left(T_J^i + T_j^{i+1}\right)}{2} \frac{\Delta Z}{\Delta t} \qquad (7)$$

in which $g_{j+1/2}$ is the mean heat gain/loss for a soil layer of thickness $\Delta Z(= 0.01 \text{ m})$ between depths j and $j + 1$ for time interval $\Delta t(= 3600 \text{ s})$ (between i and $i + 1$); Cv is the volumetric heat capacity of the layer (J K^{-1} m^{-3}); and T is the soil temperature (an average of the three locations) (K).

[20] Finally, an assessment of the quality of the complete energy balance is important. The degree of closure of the energy balance is a common approach for validating data. Complete closure ($H + E = -(NR + G)$) is rarely, if ever, attained [*Turnipseed et al.*, 2002]. A scatterplot of ($H + E$) versus ($NR + G$) together with the corresponding regression analysis is presented in Figure 4. A slope of 0.9 and a

Table 1. Closure Achievement as Has Been Reported by Several Authors

Source	Degree of Closure
Ma et al. [2003]	70%
Turnipseed et al. [2002]	75–95% with average of 85%
Tanaka et al. [2001]	70%
Anthoni et al. [2000]	70–80%
Unland et al. [1996]	mention a regression coefficient of 0.96 without any information about the slope

correlation coefficient of 0.93 were computed for the present data set. The lack of closure is most likely the result of measurement errors, probably due to the fact that each of the four fluxes was measured using a different instrument. However, when this result is compared to the degree of closure reported in the literature by others (partial list in Table 1), the degree of closure achieved in the present study can be deemed satisfactory.

4. Results and Discussion

[21] The matric potential corresponding to the maximum daily moisture content of the uppermost soil layer is less than −400 bar (computed using the *van Genuchten* [1980] formulation using the coefficients suitable to the studied soil). However, even though the matric potential of the uppermost soil layer is extremely low, a clear daily cycle of water content change in the soil can be observed. In Figure 5 the differences between total soil water content and the maximum daily total water content (mm water) are
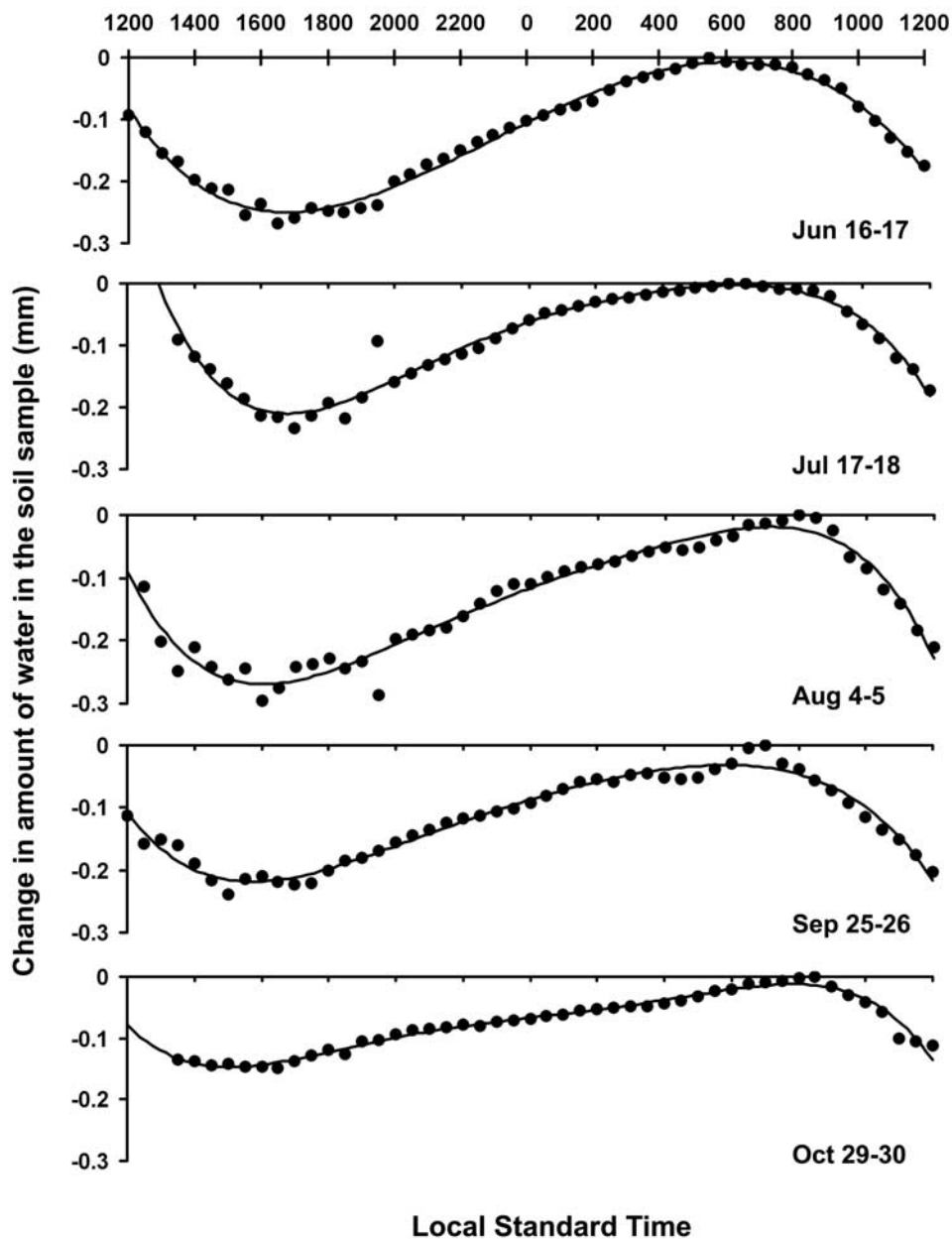

Figure 5. The differences between total soil water content and the maximum daily total water content (mm water), as measured in 16–17 June, 17–18 July, 4–5 August, 25–26 September, and 29–30 October.
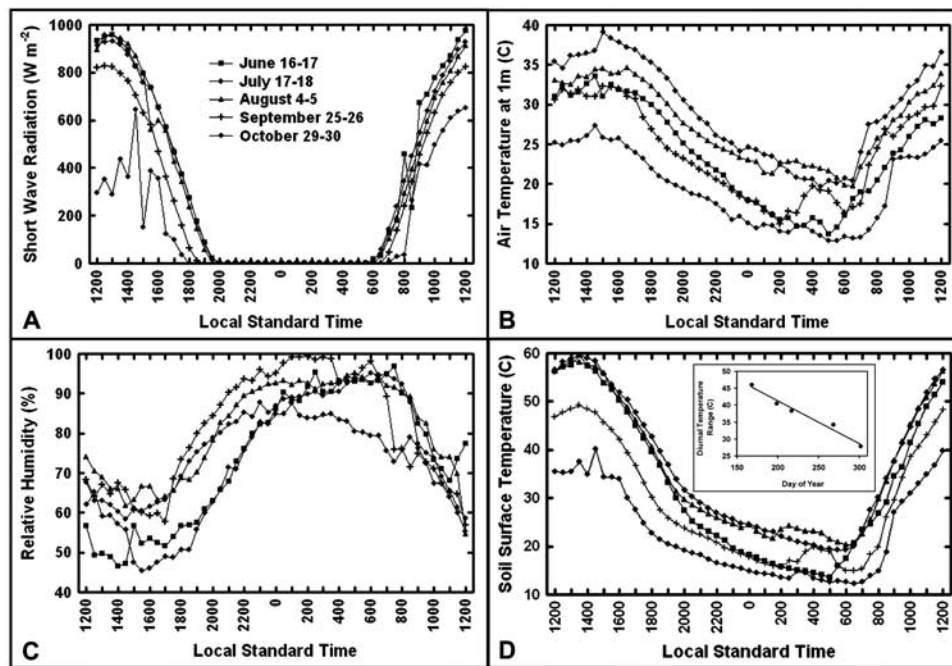
Figure 6. The daily course of important micrometeorological parameters: (a) incoming short-wave radiation, (b) air temperature, (c) relative humidity, and (d) soil-surface temperature, as measured in 16–17 June, 17–18 July, 4–5 August, 25–26 September, and 29–30 October.

presented. The largest diurnal change in the soil water content was measured in July, and the smallest in October. The soil matric potential at wilting point, which, as has been mentioned, is used in many models as the critic value for "latent heat flux shut down," is commonly set at −15 bar. For the conditions prevalent at the research site, throughout the entire dry season, the soil is drier than the wilting point and most models would predict no latent heat flux.

[22] The most important micrometeorological parameters, which are expected to affect the diurnal change in soil water content, are presented in Figure 6 for the corresponding five campaigns. The high level of short wave radiation (Figure 6a) is a characteristic of the Negev desert in which the measurements were carried out [*Berliner and Droppelmann*, 2003]. For all campaigns, except 29 October, the short wave radiation reached a maximum at ∼13:00. A very similar radiation regime can be observed for June–August, for which the highest radiation flux densities were measured, with a notable decrease in September. The abrupt course of the incoming radiation flux density during 29 October indicates that it was a cloudy day. The high levels of incoming radiation during the three first campaigns and the decrease from August to October agree well with the seasonal pattern found for the 24-hour minimum water content. In general, the higher the radiation level was, the lower was the minimum water content.

[23] The highest air temperatures were measured during the June campaign, and the lowest temperatures were measured during the October campaign (Figure 6b). Maximum air temperature was measured at ∼16:00, 3 hours later than the radiation peak. The wide peak during 29 October is the result of the presence of clouds. Minimum air temperature was monitored close to sunrise. The diurnal temperature range was large (17.18 ± 2.50°C) as can be

expected in a desert environment. No significant changes in the daily temperature range were observed for the measurement days.

[24] The daily course of the relative humidity (*RH*) (Figure 6c) has no clear seasonal trend. For all five campaigns, minimum *RH* was reached at the approximate time of the maximum air temperature (14:00–16:00). A steep increase can be observed thereafter, until midnight. During none of the nights, relative humidity reached 100%. It was very close to saturation for a few hours during the night of 25–26 September. The drier night was 17–18 July, but even during this night the *RH* was ∼90% for a short period. The fact that saturation was not reached indicates that no fog event occurred during the campaigns. There seems to be no clear correlation between the daily course of *RH* and the change in the topsoil water content.

[25] The soil surface temperature (Figure 6d) reached a daily maximum slightly later than the maximum incoming radiation (∼30 min), and slightly earlier than the minimum water content (∼30–60 min). The highest soil surface temperatures were measured during June–August. A notable decrease from August to October was observed. The ranges between maximum and minimum diurnal temperatures, for the five dates, are as well plotted in Figure 6d. Maximum range (47°C) was observed on 16–17 June (from 59.5°C at noon to 13.5°C just before sunrise). A significant decrease in the diurnal range can be seen, with a minimum of ∼28°C on 29–30 October.

[26] The components of the energy budget at the soil surface are presented in Figures 7a–7e. Fluxes directed toward the soil surface were defined as positive. Owing to instrumentation breakdown, no data of the sensible heat flux density were available for 16–17 June. The net-radiation level, during both daytime and nighttime, changed through-
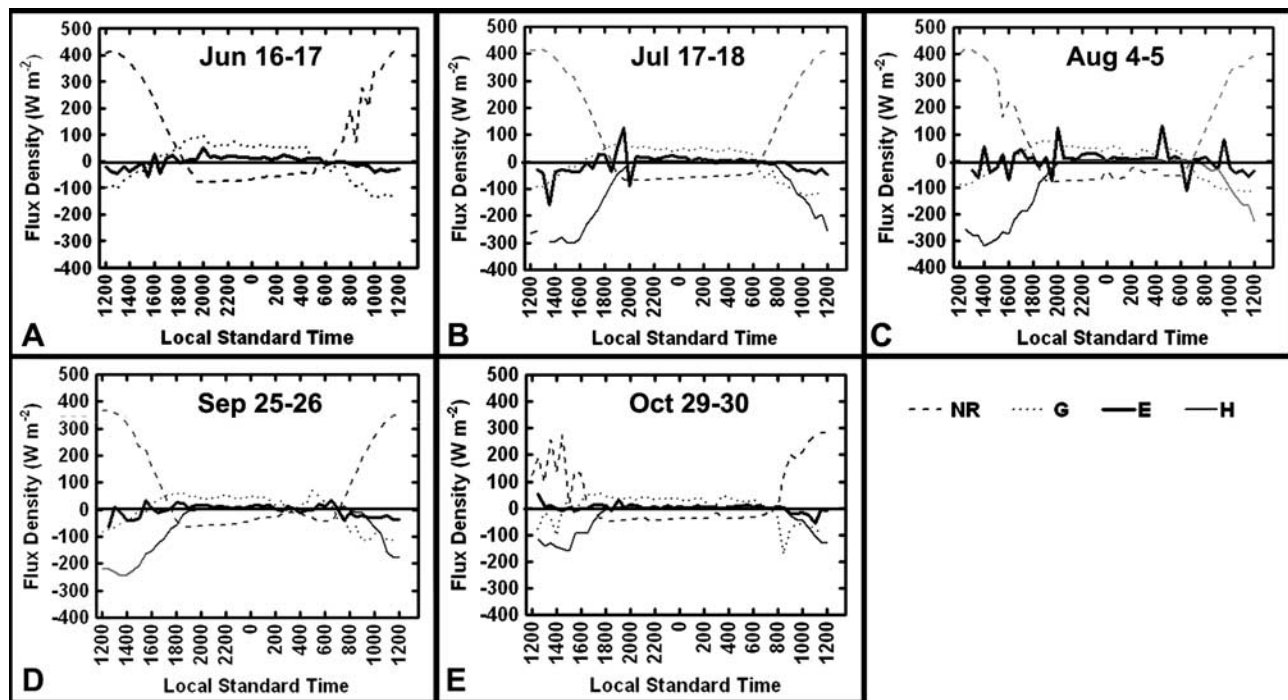
Figure 7. The daily course of the energy balance components, as measured during the five 24-hour campaigns, throughout the dry season of 2002.

out the season in a pattern similar to the one exhibited by the incoming short wave radiation, decreasing (in absolute values) from August to October. A corresponding decrease can be clearly observed for the sensible heat flux density. To a lesser extent, the same pattern can be found for the soil- and the latent- heat flux densities.

[27] It can be observed that, during daytime, a large fraction of the net-radiation was dissipated as sensible heat. However, the soil and the latent heat flux densities are not negligible. During nighttime, the soil heat flux density is the most dominant component of the energy balance, the sensible heat flux density is very small, and in most campaigns the latent heat flux density is significantly larger than the sensible one.

[28] The average values of the Bowen ratio, computed from the above-mentioned fluxes, are presented in Table 2. These values were computed for several representative hours during the day and the night for each of the campaigns. These values confirm what can be visually interpreted from Figure 7. The Bowen ratio is consistently smaller than 1 during the night, a fact that indicates that indeed the magnitude of the latent heat flux density during these hours is significantly larger than the sensible heat flux density.

[29] In order to assess the role of the latent heat flux density in the energy balance, it is necessary to compare its magnitude to the magnitude of the sensible and soil heat flux densities. Figures 8a–8e present the sensible-, latent-, and soil- heat flux densities as fractions of NR (i.e., $H + G + E = 100\%$). Since no direct measurements of sensible heat flux density were available for 16–17 June, it was derived from the energy balance equation.

[30] In the afternoon ($\sim$12:00–17:00) the sensible heat flux density is the dominant flux, being approximately 70% of the net radiation. The interesting fact is that the remaining 30% are evenly split between the latent and the soil heat flux densities (i.e., $\sim$15% each). During the late afternoon ($\sim$17:00–20:00) the sensible heat flux direction remains the same, from the soil surface toward the atmosphere. The soil heat flux direction, however, has already changed and is now directed toward the soil surface. It can be observed that while the sensible heat flux density decreases, the soil heat flux density increases. The latent heat flux density during these hours does not show a clear trend, but its magnitude remains in the range of 10–15% of the net-radiation. During the night ($\sim$20:00–06:00) the soil heat flux dominates the scene, being approximately 70% of the net-radiation. The sensible heat flux density during these hours was only about 10% of the net-radiation, and the latent heat flux density was about 20%. In the morning ($\sim$06:00–12:00) the soil heat flux changes direction and decreases gradually, while the sensible heat flux changes direction about one hour later and increases gradually. The percentage of the latent heat flux remains approximately constant, about 10–15% of the net-radiation.

5. Conclusions

[31] Measurements carried out above a loess soil in the Negev desert, during the dry season, indicated that the water

Table 2. Average Values of the Bowen Ratio: Nighttime, Daytime, and Total Averages Computed From Several Representative Hours for Each of the Dates

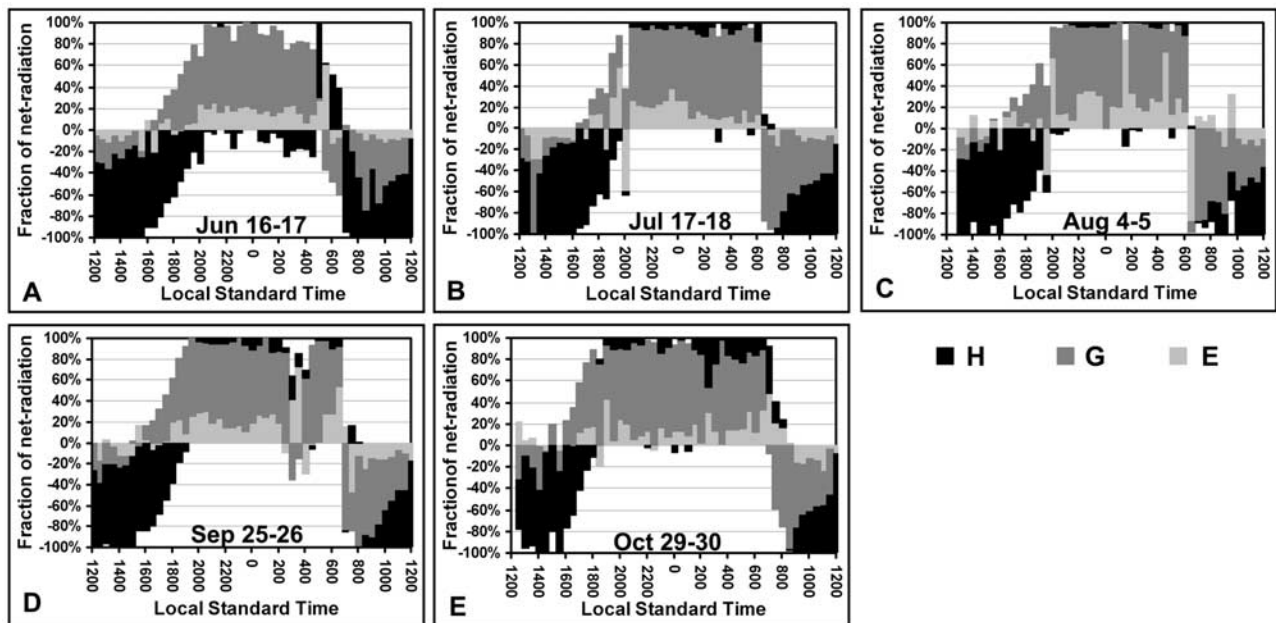| Date	Day	Night	24 Hours
17–18 July	6.89	0.33	3.08
5–6 Aug.	7.08	0.16	3.39
25–26 Sept.	8.83	0.49	4.12
29–30 Oct.	6.75	0.91	3.28
Average	7.39	0.47	3.47

Figure 8. The soil- (*G*), sensible- (*H*), and latent- (*E*) heat flux densities as fractions of the net-radiation (*NR*) (i.e., *H* + *G* + *E* = 100%), as measured during the five 24-hour campaigns. Note that the sensible heat flux density during 16−17 June was derived from the energy balance equation.

content of the uppermost soil layer reach values that are significantly and systematically lower than the wilting point. Most of the commonly used meteorological models would therefore assume no latent heat flux. Nevertheless, latent heat flux densities were monitored throughout the dry season.

[32] Latent heat flux density reaches ∼20% of the net-radiation during the night, and thus plays a major role in the dissipation of the net radiation. However, it should be kept in mind, that the overall flux densities at night are rather small. The 10−15% of the net-radiation during the day is even more significant as the magnitude of the flux densities is much larger. It is thus clear that models that assume that during the dry season there is no latent heat flux over deserts may lead to erroneous results.

References

Agam (Ninari), N., and P. R. Berliner (2004), Diurnal water content changes in the bare soil of a coastal desert, *J. Hydrometeorol*, in press.

Anthoni, P. M., B. E. Law, M. H. Unsworth, and R. J. Vong (2000), Variation of net radiation over heterogeneous surfaces: measurements and simulation in a juniper-sagebrush ecosystem, *Agric. For. Meteorol.*, *102*(4), 275−286.

Avissar, R., and R. A. Pielke (1989), A parameterization of heterogeneous land surfaces for atmospheric numerical models and its impact on regional meteorology, *Mon. Weather Rev.*, *117*, 2113−2136.

Berliner, P. R., and K. J. Droppelmann (2003), Validation in an aid area of an algorithm for the estimation of daily solar radiation, *J. Hydrometeorol.*, *4*, 297−303.

Blondin, C. (1991), Parameterization of land-surface processes in numerical weather prediction, in *Land Surface Evaporation—Measurement and Parameterization*, edited by T. J. Schmugge and J.-C. Andre, pp. 31−54, Springer-Verlag, New York.

Bougeault, P. (1991), Parameterization schemes of land-surface processes for mesoscale atmospheric models, in *Land Surface Evaporation—Measurement and Parameterization*, edited by T. J. Schmugge and J.-C. Andre, pp. 55−92, Springer-Verlag, New York.

Boulet, G., I. Braud, and M. Vauclin (1997), Study of the mechanisms of evaporation under arid conditions using a detailed model of the soil-atmosphere continuum: Application to the EFEDA I experiment, *J. Hydrol.*, *193*(1−4), 114−141.

Brutseart, W. (1982), *Evaporation Into the Atmosphere*, D. Reidel, Norwell, Mass.

Carlson, T. N., F. G. Rose, and E. M. Perry (1984), Regional-scale estimates of surface moisture availability from GEOS infrared satellite measurements, *Agron. J.*, *76*(6), 972−979.

Chen, F., and J. Dudhia (2001), Coupling an advanced land surface–hydrology model with the Penn State–NCAR MM5 modeling system. part I: Model implementation and sensitivity, *Mon. Weather Rev.*, *129*, 569−585.

European Centre for Medium-Range Weather Forecasts (2002), Integrated Forecast System, Reading, UK.

Gusev, Y. M., and O. N. Nasonova (2003), The simulation of heat and water exchange in the boreal spruce forest by the land-surface model SWAP, *J. Hydrol.*, *280*(1−4), 162−191.

Hu, Z., and S. Islam (1997), Effects of spatial variabilities on the scaling of land surface parameterizations, *Boundary Layer Meteorol.*, *83*, 441−461.

Irannejad, P., and Y. Shao (1998), Description and validation of the atmosphere-land-surface interaction scheme (ALSIS) with HAPEX and Cabauw data, *Global Planet. Change*, *19*(1−4), 87−114.

Kondo, J., N. Saigusa, and T. Sato (1990), A parameterization of evaporation from bare soil surfaces, *J. Appl. Meteorol.*, *29*, 385−389.

Lohmann, D., D. P. Lettenmaier, X. Liang, E. F. Wood, A. Boone, S. Chang, F. Chen, Y. Dai, C. Desborough, and R. E. Dickinson (1998), The Project for Intercomparison of Land-surface Parameterization Schemes (PILPS) phase 2 (c) Red-Arkansas River basin experiment: 3. Spatial and temporal analysis of water fluxes, *Global Planet. Change*, *19*(1−4), 161−179.

Ma, Y., Z. Su, T. Koike, T. Yao, H. Ishikawa, K. I. Ueno, and M. Menenti (2003), On measuring and remote sensing surface energy partitioning over the Tibetan Plateau—From GAME/Tibet to CAMP/Tibet, *Phys. Chem. Earth, Parts A/B/C*, *28*(1−3), 63−74.

Milly, P. C. D. (1982), Moisture and heat transport in hysteretic, inhomogeneous porous media: A matric-based formulation and a numerical model, *Water Resour. Res.*, *18*(3), 489−498.

Milly, P. C. D. (1984), A simulation analysis of thermal effects on evaporation from soil, *Water Resour. Res.*, *20*(8), 1087−1098.

Mitsuta, Y., I. Tamagawa, K. Sahashi, and J. Wang (1995), Estimation of annual evaporation from the Linze desert during HEIFE, *J. Meteorol. Soc. Jpn.*, *73*, 967−974.

Ninari, N., and P. R. Berliner (2002), The role of dew in the water and heat balance of bare loess soil in the Negev Desert: Quantifying the actual dew deposition on the soil surface, *Atmos. Res.*, *64*(1−4), 323−334.

Parlange, M. B., A. T. Cahill, D. R. Nielsen, J. W. Hopmans, and O. Wendroth (1998), Review of heat and water movement in field soils, *Soil Tillage Res.*, *47*(1−2), 5−10.

Philip, J. R., and D. A. de Vries (1957), Moisture movement in porous materials under temperature gradients, *Eos Trans. AGU*, *38*(2), 222−232.

Qin, Z., P. Berliner, and A. Karnieli (2002), Numerical solution of a complete surface energy balance model for simulation of heat fluxes and surface temperature under bare soil environment, *Appl. Math. Comput.*, *130*(1), 171−200.

Robock, A., C. A. Schlosser, K. Y. Vinnikov, N. A. Speranskaya, and J. K. Entin (1998), Evaluation of AMIP soil moisture simulations, *Global Planet. Change*, *19*, 181−208.

Scanlon, B. R., and P. C. D. Milly (1994), Water and heat fluxes in desert soils: 2. Numerical simulations, *Water Resour. Res.*, *30*(3), 721−733.

Schmugge, T. J., and J.-C. Andre (1991), *Land Surface Evaporation— Measurement and Parameterization*, 424 pp., Springer-Verlag, New York.

Shao, Y., and A. Henderson-Sellers (1996), Validation of soil moisture simulation in land surface parameterization schemes with HAPEX data, *Global Planet. Change*, *13*(1−4), 11−46.

Sridhar, V., R. L. Elliott, and F. Chen (2003), Scaling effects on modeled surface energy-balance components using the NOAH-OSU land surface model, *J. Hydrol.*, *280*(1−4), 105−123.

Tanaka, K., H. Ishikawa, T. Hayashi, I. Tamagawa, and Y. M. Ma (2001), Surface energy budget at Amdo on the Tibetan Plateau using GAME/ Tibet IOP98 data, *J. Meteorol. Soc. Jpn.*, *79*(1B), 505−517.

Turnipseed, A. A., P. D. Blanken, D. E. Anderson, and R. K. Monson (2002), Energy budget above a high-elevation subalpine forest in complex topography, *Agric. For. Meteorol.*, *110*(3), 177−201.

Unland, H. E., P. R. Houser, W. J. Shuttleworth, and Y.-L. Zong (1996), Surface flux measurement and modeling at a semi-arid Sonoran Desert site, *Agric. For. Meteorol.*, *82*(1−4), 119−153.

van Genuchten, M. T. (1980), A closed-form equation for predicting the hydraulic conductivity of unsaturated soils, *Soil Sci. Soc. Am. J.*, *44*, 892−898.

Yang, Z.-L., and R. E. Dickinson (1996), Description of the Biosphere-Atmosphere Transfer Scheme (BATS) for the Soil Moisture Workshop and evaluation of its performance, *Global Planet. Change*, *13*(1−4), 117−134.

Yang, Z.-L., R. E. Dickinson, W. J. Shuttleworth, and M. Shaikh (1998), Treatment of soil, vegetation and snow in land surface models: A test of the Biosphere-Atmosphere Transfer Scheme with the HAPEX-MOBILHY, ABRACOS and Russian data, *J. Hydrol.*, *212−213*(1−4), 109−127.

―――――――――――

N. Agam (Ninari), P. R. Berliner, and A. Zangvil, Jacob Blaustein Institute for Desert Research, Ben-Gurion University of the Negev, Sede-Boker Campus, 84990, Israel. (agam@bgumail.bgu.ac.il)

E. Ben-Dor, Remote Sensing and GIS Laboratory, Department of Geography, Tel-Aviv University, Ramat Aviv, P.O. Box 39040, Tel-Aviv, 69978, Israel.